

**SHOCK-INDUCED TRANSFORMATIONS IN OLIVINE OF THE CHASSIGNITE NWA 2737** B. Reynard, B. Van de Moortèle, P. Beck, P. Gillet, Laboratoire de Sciences de la Terre, Ecole Normale Supérieure de Lyon, 46 Allée d'Italie, 69007 Lyon, France (e-mails: [bruno.reynard@ens-lyon.fr](mailto:bruno.reynard@ens-lyon.fr), [bvandemo@ens-lyon.fr](mailto:bvandemo@ens-lyon.fr), [pbeck@ens-lyon.fr](mailto:pbeck@ens-lyon.fr), [pgillet@ens-lyon.fr](mailto:pgillet@ens-lyon.fr))

The petrology and geochemistry of Northwest Africa 2737 (NWA 2737), a Martian meteorite found in the Moroccan Sahara in 2000, make it the second member of the chassignites [1]. This rock is a cumulate consisting in black olivine- and spinel-cumulate crystals (89.7 and 4.6 wt% respectively), with intercumulus pyroxenes (augite 3.1 wt% and pigeonite-orthopyroxene 1.0 wt%), sanidine glass (1.6 wt.%) and apatite (0.2 wt%). Unlike Chassigny, plagioclase has not been observed in NWA 2737.

The black color of Mg-rich and highly equilibrated (Fo<sub>79</sub>) olivine grains, giving its very dark aspect to the rock, is intriguing and at contrast with the light color of more iron-rich (Fo<sub>69</sub>) olivine of Chassigny.

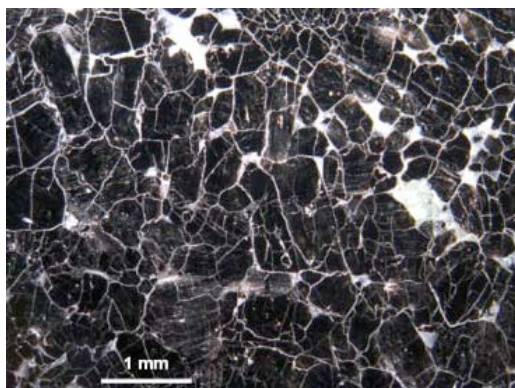


Fig. 1: Optical micrograph of a polished section of NWA 2737 showing the dominant olivine phase appearing generally dark grey to black, and exceptionally with its "normal" greenish transparent aspect. White patches are pyroxenes and maskelynite. White tiny veins at grain boundaries are filled with carbonates.

In order to elucidate these optical properties, we studied them by Raman spectroscopy using a Jobin-Yvon LabRaman spectrometer, and an Ar<sup>+</sup> laser (514 nm) for excitation. The size of the laser spot onto the sample was around  $\sim 2 \mu\text{m}$ . Transmission electron microscopy (TEM) and high resolution images (HRTEM) were obtained on a Jeol 2010F microscope, operating at 200 kV, and equipped for the chemical nano-analysis (probe size typically 2 nm for the investigation of nanometric features) with an EDX analyzer (Inca Oxford). The EDX calibration was checked by the analysis of a thin foil of San Carlos olivine which composition was first measured by electronic microprobe analysis (EMPA). Accuracy is about 0.5 atom%.

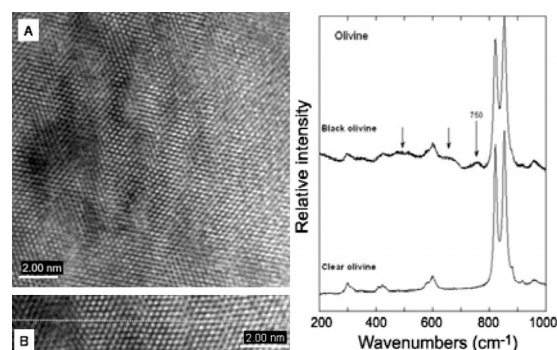


Fig.2: HRTEM image (left) and Raman spectrum (right) of black olivine. Fourier transforms (FT) of the HRTEM images cannot be indexed within the olivine orthorhombic lattice, but are consistent with a hexagonal compact packing (hcp) lattice with parameter of  $\sim 0.3 \text{ nm}$ . This is similar to transformations observed in olivines at pressures between 40 and 70 GPa and low ( $< 1000 \text{ K}$ ) temperatures [2]. Raman spectra of the dark olivines show extra peaks near 670 and 750  $\text{cm}^{-1}$ , which can be attributed to the formation of Si-O-Si bridges. Similar transformations are observed at ambient temperature and at pressures above 50 GPa in forsterite [3] and above 10 GPa in germanate olivines [4,5]. They are interpreted as hindered transitions towards olivine high pressure polymorphs.

Raman and HRTEM observations (Fig. 2) point to pressure-induced transformations, which we attribute to the shock that extracted the meteorite from Mars. These transformations did not lead to the formation of the stable high-pressure polymorphs of olivine, but to intermediate states where the olivine structure is disordered. Such states are observed in experiments where the temperatures are too small to allow significant diffusion-controlled reconstructive transformations to take place. This observation is at variance of those on Chassigny where only mosaicism and fracturation has been reported in olivines [6]. In addition to the above transformations, many areas of the dark olivines display tiny inclusions of less than 20 nm in diameter. In order to decipher the structure, number and chemistry of these inclusions, both annular dark field imaging, HRTEM and nano-EDX analyses were used (Figs 3 and 4). The density of inclusions is about 0.1% in volume. First results suggest that their chemistry is that of FeNi alloy, which stoichiometry depends on the size of the inclusion. The smaller the inclusion, the higher the Ni/Fe ratio.

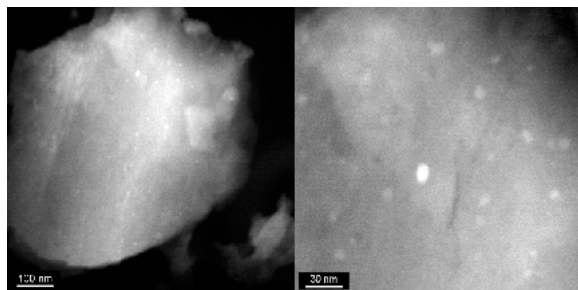


Fig. 3: Annular dark field images of black olivines. This imaging mode enhances density contrast and reveals the presence of dense nanophases in the olivine grain shown here. The size of these particles is less than 20 nm. Estimated density is one particle per  $10^6 \text{ nm}^3$ , i. e. no more than 0.1% in volume.

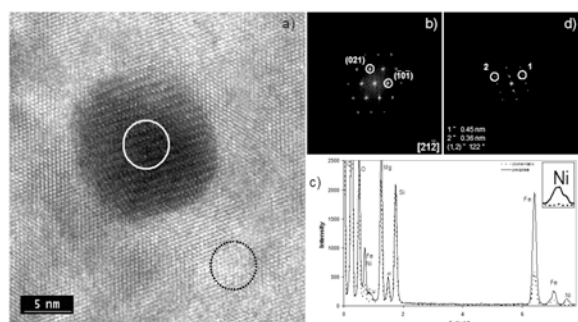


Fig. 4: HRTEM image and EDX analysis of a dense nanoparticle in olivine. Analyses are performed on the matrix alone (dotted circle) and on the inclusions within the matrix (white circle). Resolution of the analyses in two components (matrix olivine + inclusions) shows that the nanoparticle is  $\text{Fe}_{93}\text{Ni}_7$  metal alloy, likely precipitated by partial reduction of the host olivine. Reduction of the olivine is consistent with the strong Ni enrichment in the inclusion (7% here and up to 30% in smaller precipitates) with respect to the bulk olivine (around 900 ppm from EMPA). FT of the matrix can be indexed within the olivine lattice, and FT on the inclusion show extra spots, which could not be successfully indexed in any known metal phase. Given the small size of the inclusion (7-8 nm in diameter), it is possible that its atomic arrangement is strongly influenced by the matrix.

The presence of numerous and tiny metallic inclusions can account for the color of the olivine and rock. It is worth noting that the occurrence of metallic nanoparticle is uncommon in planetary materials, as it is more commonly observed in primitive meteorites and as a result of space weathering. Another noticeable characteristic is that reduced metal is formed without production of either pyroxene or amorphous silica rich phase around metallic inclusions, which is required for the balance of the reduction. This may be explained either by the

small quantity of metal formed, which could be accommodated within the non-stoichiometry of olivine. All structural and chemical observations suggest that these inclusions formed under reducing conditions, in order to account for their metallic nature and their enrichment in Ni with respect to the host olivine. Because the magmatic history of this dunite takes place under relatively oxidizing conditions estimated around or above the fayalite-magnetite-quartz (FMQ) buffer, the metallic inclusions have to form by subsolidus reduction of the olivine. This can take place at two moments in the history of the rock: 1) by reduction during the subsolidus cooling of the rock or 2) during the shock event that partially transformed olivine (Fig. 2) and caused the formation of maskelynite from alkali feldspar [1]. The first scenario is unlikely because the rock emplaced, like Chassigny, at shallow level in the Martian crust [7] which is rather oxidized than reduced. Reduction during the shock can be achieved at constant oxygen fugacity (or at constant composition) if the temperature during the shock exceeds that of the magmatic equilibration. Using magmatic equilibration temperatures of  $1070^\circ\text{C}$  obtained from olivine-augite Fe/Mg equilibrium near FMQ and assuming that iron precipitation will take place around the iron-wüstite buffer, we estimate a required temperature of about  $1300^\circ\text{C}$  at ambient pressure, which could represent a residual temperature for the shock. Precipitation of the metal nanoparticles requires interdiffusion of Mg, Fe and Ni over characteristic distances of 100 nm. Given the above estimate for temperature and available diffusion coefficients [8,9], this can be achieved within less than 10 ms. This time scale is of the same order of magnitude as recent estimate for shock durations in Martian meteorites [10].

**References:** [1] Beck P. et al. (2006) GCA, in the press. [2] Guyot F. and Reynard B. (1992) Chem Geol, 96, 411-420. [3] Durben D. J. et al. (1993) Am Mineral, 78, 1143-1148. [4] Reynard B. et al. (1994) Phys Chem Minerals, 20, 556-562. [5] Reynard B. et al. (1997) Phys Chem Minerals, 24, 77-84. [6] Langenhorst F and Greshake (1999) M&PS, 34, 43-48. [7] Mikouchi et al. (2005) LPSC XXXVI, Abst. #1944. [8] Buening D. K. and Buseck P. R. (1973), JGR, 78, 6852-6862. [9] Petry C. et al. (2004), 68, 4179-4188. [10] Beck P. et al. (2005), Nature, 435, 1071-1074.

**Acknowledgments.** Consortium LYonnais de Microscopie Electronique (CLYME) is thanked for access to TEM facilities. This work was funded by CNRS and Région Rhône-Alpes program Emergence.